PROCEEDINGS OF THE ROYAL SOCIETY A

Proc. R. Soc. A (2010) **466**, 157–175
doi:10.1098/rspa.2009.0412
Published online 2 October 2009

The application of enzyme reaction, nonlinear diffusion models to the malting process

By Neville Fowkes[1,*] and Ricky O'Brien[2]

[1]*School of Mathematics and Statistics, The University of Western Australia, Crawley, Western Australia 6009, Australia*
[2]*EOS Space Systems Pty Ltd, 111 Canberra Avenue, Griffith, ACT 2603, Australia*

We extend the classic Michaelis–Menten kinetics model of the enzyme-mediated conversion of substrate to product to situations in which the enzymes need to diffuse through the underlying structure to reach unconverted substrate and in which the diffusivity is greatly increased by the conversion. The work was prompted by the study of the germination and modification of barley grain that occurs during malting, but is broadly applicable. A nonlinear diffusion, enzyme reaction model of the modification process is proposed and some accurate approximate analytic solutions are derived. We find that a sharp modification front is set up between the modified and the unmodified regions of the barley grain. This front propagates with an almost constant speed through the medium and our findings are consistent with the available experimental observations.

Keywords: enzyme kinetics; reaction diffusion; modification; germination

1. Introduction

Two reacting chemical species, one in fluid form and the other a solid, will combine as the fluid diffuses through the underlying solid matrix structure. If the effect of the reaction is to significantly change the diffusive properties of the matrix, then the conversion rate and the penetration speed will be joint functions of both the chemistry and the consequent structural change in the solid. This combination may be enough to close down the reaction, as in the case of the oxidation of aluminium, or it might open up the matrix enabling the reaction to proceed at close to the maximum rate associated with perfectly mixed and powdered samples. Ablation is an analogous state change process with a most dramatic structural change from solid to gas, and in this case a constant speed front is often set up. The structural change brought about by melting is not quite so dramatic and results in a front that typically travels with a speed inversely proportional to the square root of time (as in the Neumann solution). In this paper, we examine a biological situation which involves an enzymic reaction that seemingly could not proceed without the accompanying structural change in the substrate. We will focus on a problem arising in the malting of barley for definiteness, although it is to be hoped that our results are more widely applicable.

*Author for correspondence (fowkes@maths.uwa.edu.au).

Received 7 August 2009
Accepted 3 September 2009

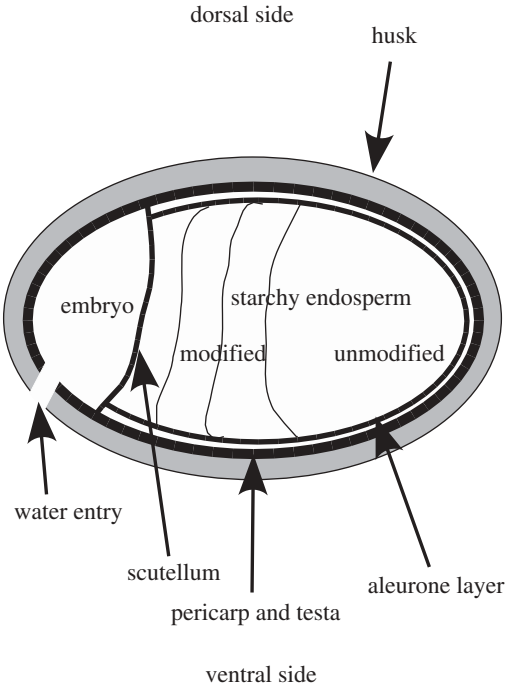

Figure 1. Patterns of modification in the barley grain. A front propagates from the proximal (left hand) to the distal (right hand) end of the grain. Taken from Oh & Briggs (1989).

Malsters attempt to create ideal conditions for the germination of barley grains by maintaining a light, warm, moist and well-aerated environment. Germination produces the enzymes required for the modification of the endosperm of the grain, and the production of sugar from starch. A schematic of the process of germination is shown in figure 1. Gibberellic acid is released by the awakened embryo and diffuses into the aleurone layer surrounding the endosperm. The acid triggers the production of enzymes that subsequently diffuse across the layer of cells separating the aleurone and the endosperm. Many different enzymes are produced but they can all be identified as belonging to one of the two distinct families: the first of these comprise the β-glucanases, which break up glutin chains in the cell walls that encase starch granules within the endosperm. The starch molecules are thus exposed to the action of the so-called α and β amylases, the second family, which act on the released starch to produce the sugars required for acrospire and root growth and alcohol production. More details can be obtained from Bamforth & Martin (1983) or Selvig *et al.* (1986).

One action of the glucanases is to cause a rather dramatic change in the structural composition of the endosperm. In its original form, the endosperm is structurally strong and virtually impermeable, whereas its modified state is both friable and permeable. This significant change in physical properties means that staining techniques can be used to follow the temporal pattern of the modification. Experiments seem to suggest that the two states are separated by a sharp front

which travels with approximately uniform speed and that, although the time required for complete modification does vary with species, it averages out at about 5 days. Figure 1 shows how a typical modification pattern develops and how the front propagates from the proximal to the distal end of the grain (Oh & Briggs 1989). We remark that other experimentalists have reported other patterns of modification (e.g. Briggs & MacDonald 1983 or Palmer 1983) and these have been discussed elsewhere (O'Brien & Fowkes 2005). Here, our interest is rather with a determination of the front speed and structure in terms of basic physical and chemical parameters.

We address this issue by using an adapted Michaelis–Menten enzyme kinetics model. The original Michaelis–Menten system was proposed as a model to describe how enzymes generate a product from a substrate under uniform mixing conditions but here we need to take account of the highly nonlinear diffusion effects arising from the significant alteration in the structure of the endosperm that occurs as the germination proceeds. In §2, we develop our model equations and reduce them to their simplest form. Some numerical simulations described in §3 display how the front develops and propagates. These results motivate some analytical work which leads to approximate (though surprisingly accurate) solutions for the parameter ranges of interest. Simple expressions for the front thickness and propagation speed are extracted and the results obtained are compared with some published experimental and observational results for barley modification. We conclude in §4 with some comments concerning the strengths and weaknesses of the model.

2. The enzyme reaction–nonlinear diffusion model

The family of Michaelis–Menten models typically involve a reaction in which some enzyme E converts a substrate S into a product P through a two-stage process. In the first stage, the substrate combines with the enzyme to form a complex C, which in the second stage breaks down into the product while simultaneously releasing the enzyme. This can be represented schematically by

$$S + E \rightleftharpoons C \longrightarrow P + E. \tag{2.1}$$

Using $s(t)$, $c(t)$, $e(t)$ and $p(t)$ to denote the spatially uniform concentrations of the above components as a function of time, Briggs & Haldane (1925) modelled the enzyme reaction by

$$\frac{\mathrm{d}s}{\mathrm{d}t} = k_{-1}c - k_1 se, \quad \frac{\mathrm{d}e}{\mathrm{d}t} = (k_{-1} + k_2)c - k_1 se \tag{2.2}$$

and

$$\frac{\mathrm{d}c}{\mathrm{d}t} = k_1 se - (k_2 + k_{-1})c, \quad \frac{\mathrm{d}p}{\mathrm{d}t} = k_2 c, \tag{2.3}$$

where the k_j are positive rate constants.

To relate this system to barley modification, it is known that β-glucanase molecules (e) attach to glucan chains (s) forming a complex (c), which then breaks up leaving broken glucan chains (p) and releasing the enzyme (e); hence the s and p concentration levels can be identified with the number of unbroken and broken glucan links per unit volume, respectively. In practice, water is required for

the above process to proceed but the time scale for the diffusion of water over the length of the grain is very much less than the modification time, so the reaction can safely be assumed to take place within a uniform moisture environment, see Landman & Please (1999) or McGuinness *et al.* (2000). We will also assume a fixed temperature environment.

Systems (2.2) and (2.3) cannot legitimately be used as a model of grain modification for it assumes that the reaction components are well mixed. It is known that the modification within a grain of barley proceeds at an order of magnitude slower than would be seen if the reactants were properly mixed (with powdered grain, the reaction occurs in hours rather than days) so it is evident that transport processes play a key role in modification. Both the product and the substrate remain fixed in position within the starch matrix, so that mobile enzymes must diffuse from an input source (the aleurone and possibly the scutellum layers) to the reaction site before the complex formation and breakdown reactions can proceed. The complexed enzymes are (temporarily) immobilized so that we include an enzyme diffusion term in the model equations (2.2) and (2.3) to give the extended model

$$\frac{\partial s}{\partial t} = k_{-1}c - k_1 se, \tag{2.4}$$

$$\frac{\partial e}{\partial t} = \nabla \cdot (D(s)\nabla e) + (k_{-1} + k_2)c - k_1 se, \tag{2.5}$$

$$\frac{\partial c}{\partial t} = k_1 se - (k_{-1} + k_2)c \tag{2.6}$$

and

$$\frac{\partial p}{\partial t} = k_2 c, \tag{2.7}$$

where ∇ is taken with respect to the relevant spatial coordinates.

To proceed further we need to say rather more about the nature of the substrate-dependent diffusion coefficient $D(s)$. Enzyme molecules are typically large (a molecular weight $O(10^5)$ is common) and the matrix formed by unmodified endosperm is dense, so that one would expect very small diffusitivity levels in the unmodified endosperm with a large increase occurring after cell wall breakdown. The fact that staining techniques (which use small molecules) sharply mark out the modification zone is consistent with this ansatz. We therefore take $D = D(s)$ to be a rapidly decreasing function of s and for the remainder of this study an exponential dependence

$$D(s) = D_0 \exp(\mu(s_0 - s)) \tag{2.8}$$

is assumed, where s_0 is the initial substrate concentration and μ is a constant with μs_0 moderate to large. Some rough estimates for a few of the physical and chemical parameters can be deduced for the germination of barley problem and these are discussed below in §3*d*. In the meantime, we proceed using parameter values that are both reasonable and best display the important solution features.

(*a*) *Scaling and model simplification*

Enzyme concentration levels are normally very small compared with the substrate and product concentration levels: ratios of the order of 10^{-6} are quite typical. During the modification process, one might expect almost all available enzymes to be engaged in composite formation so that enzyme and composite concentrations are likely to be comparable. The appropriate scalings for species concentration levels are thus given by

$$s = s_0\bar{s}, \quad e = e_0\bar{e}, \quad c = e_0\bar{e} \quad \text{and} \quad p = s_0\bar{p}, \quad \text{where } \varepsilon = e_0/s_0 \ll 1, \tag{2.9}$$

in which s_0 denotes the initial substrate concentration in the endosperm and e_0 is the maximum enzyme concentration level around its boundary. In our barley process, enzymes are synthesized from molecules already present within the aleurone layer so the relative volume of that layer to the volume occupied by glucan cell walls in the endosperm provides an overestimate for ε of $O(10^{-5})$.

There are three important time scales in the problem. The first is the substrate conversion time τ_0 defined by $\tau_0 = 1/(k_1 e_0)$, see equation (2.4), which determines the time scale required for the conversion of substrate to complex. Estimates suggest $\tau_0 \sim 1$ h. Next is the complex adjustment time $\tau_c = 1/(k_1 s_0) = \varepsilon\tau_0$, which is the period over which the complex concentration adjusts to changes in enzyme concentration. This is very much smaller than τ_0, and τ_c is roughly the order of a few milliseconds; it is the rapid and repeated recycling that results in the overall large-scale conversion of the substrate. Last comes the diffusion time $\tau_d \equiv L^2/D(s_0)$, where L is a characteristic length scale of the modification zone which here is taken to be the length of the grain. The diffusion time scale is very much greater than the other two and τ_d is likely to be of the order of a few weeks.

Our three time scales each play some active role in the modification process and the fact that they differ by orders of magnitude means that asymptotic analysis is required to obtain a proper understanding of the process. It is useful to adopt L as our length scale, and to scale t using the substrate conversion time τ_0. Also, it is convenient to replace the enzyme conservation equation (2.5) by the total (free plus complexed) enzyme conservation equation. With the above scales and this rearrangement, systems (2.4)–(2.7) reduces to

$$\frac{\partial s}{\partial t} = Rc - se, \quad \frac{\partial}{\partial t}(e + c) = D\nabla \cdot (e^{\beta(1-s)}\nabla e) \tag{2.10}$$

and

$$\varepsilon\frac{\partial c}{\partial t} = se - \kappa c, \quad \frac{\partial p}{\partial t} = V_{max}c \tag{2.11}$$

(after dropping the bar notation), where $D \equiv D_0/(L^2 e_0 k_1)$, $V_{max} \equiv k_2/(s_0 k_1)$, $R \equiv k_{-1}/(k_1 s_0)$, $\beta \equiv \mu s_0$ and $\kappa \equiv V_{max} + R$. We subsequently refer to this equation set as our complete model.

Under spatially uniform conditions, the diffusion term vanishes and the familiar Michaelis–Menten equations are recovered. The behaviour of this simplified system is well known: after a time scale of $O(\varepsilon)$, the system settles into a pseudo-steady state in which the rate of formation of the complex is balanced by its rate of breakdown. The concentration of the complex is thus

determined by the enzyme and substrate concentration levels according to the equilibrium condition

$$se = \kappa c, \tag{2.12}$$

obtained at leading order by simply ignoring the (small) derivative term in (2.11a). In our present problem, we would expect local complex concentration levels to adjust quickly to local enzyme and substrate concentration levels according to this equilibrium condition with the subsequent conversion governed by this equation together with

$$\frac{\partial s}{\partial t} = -\mathcal{K} se, \quad \frac{\partial}{\partial t}(e + c) = D\nabla \cdot (e^{\beta(1-s)}\nabla e), \tag{2.13}$$

where

$$\mathcal{K} \equiv \frac{\kappa - R}{\kappa} = \frac{k_2}{k_2 + k_{-1}}$$

and where we have used the complex equilibrium condition (2.12) to simplify the substrate conversion equation (2.10a). We can now remove one more parameter from our formulation by re-adjusting the time scale using $t = t'/\mathcal{K}$. What remains is the pseudo-steady model

$$\frac{\partial s}{\partial t} = -se, \tag{2.14}$$

$$\frac{\partial (e + c)}{\partial t} = D_r \nabla \cdot (e^{\beta(1-s)}\nabla e) \tag{2.15}$$

and

$$se = \kappa c, \tag{2.16}$$

where $D_r \equiv D/\mathcal{K}$, and we have dropped the dash on t. We note that the adopted time scale is such that $s = \exp(-t)$ under uniform ($e = 1$) conditions and so can be interpreted to be the total reaction time scale τ_r under uniform conditions.

Our final model contains a couple of significant dimensionless groupings. The scaled diffusivity $D_r = \tau_r D_0/L^2 \equiv \tau_r/\tau_d$ is the diffusivity of the unmodified endosperm based on reaction time scale τ_r and the length scale of the zone of modification L. Equivalently, it is the ratio of the reaction time scale to the diffusion time scale: as such, we expect D_r to be very small and for the purposes of later illustration $D_r = 10^{-3}$ will be used. The diffusivity variation parameter β determines the relative change in diffusivity brought about by the reaction. It is the modification of the substrate that enables the reaction to proceed at moderate speed, so we expect the scaled diffusivity of the modified material, $D_r e^{\beta}$, to be of order one or larger, so β needs to be reasonably large. For definiteness, we use $\beta = 6$, so that the scaled diffusivity range is 0.001–0.4.

3. The propagating front

For circumstances of interest, enzymes are introduced into the substrate around a boundary surface and diffuse into and react with the substrate along a propagating front, leaving product in its wake. We will endeavour to estimate the propagation speed and structure of the front for a semi-infinite slab $x > 0$. Enzyme input is supposed to take place at the face $x = 0$ and, in order to assess the validity of the pseudo-steady model, we study both the full equation set

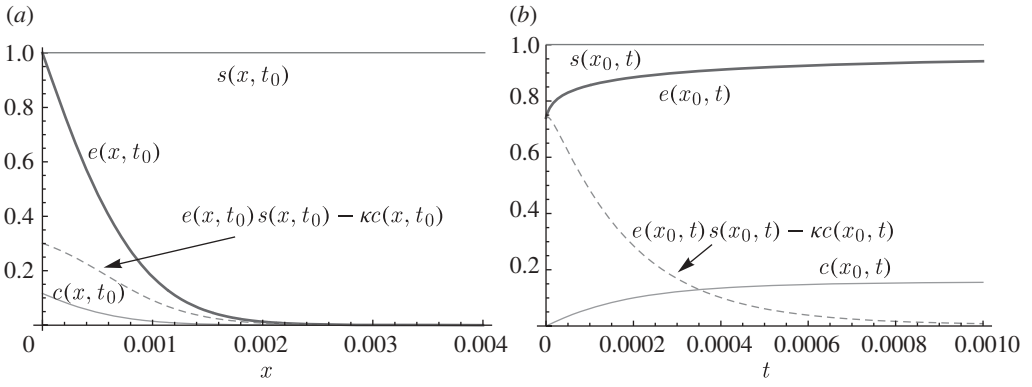

Figure 2. Small-time solution behaviour of the complete model equations. (*a*) Spatial distributions $e(x, t_0)$ (thick curve), $s(x, t_0)$ (medium curve), $c(x, t_0)$ (thin curve) and $s(x, t_0)e(x, t_0) - \kappa\, c(x, t_0)$ (dashed curve) at time $t_0 = 2 \times 10^{-4}$. (*b*) Temporal functions $e(x_0, t)$ (thick curve), $s(x_0, t)$ (medium curve), $c(x_0, t)$ (thin curve) and $s(x_0, t)e(x_0, t) - \kappa\, c(x_0, t)$ (dotted curve) at location $x_0 = 10^{-4}$. Parameter values fixed as $\varepsilon = D_r = 10^{-3}$ and $\beta = \kappa = 6$.

(2.10) and (2.11) and the pseudo-steady system (2.14)–(2.16). Initial conditions are that $s(x, 0) = 1$ and $e(x, 0) = 0$ and we suppose that the enzyme concentration at the face $x = 0$ is held at the constant value $e(0, t) = 1$ in dimensionless terms. In the case of the full system, we also need to specify the initial distribution of the complex and take $c(x, 0) = 0$.

An iterative implicit finite difference scheme was used to integrate this stiff system. Accurate numerical simulations were obtained for a broad range of parameters with D_r ranging from 10^{-6} to 10^{-1}, ε from 10^{-1} to 10^{-5}, β either zero or $\beta \in [2, 10]$ and $\kappa \in [2, 6]$. A small but representative selection of the results obtained will be presented here; for a more complete set the interested reader is directed to O'Brien (2004).

(*a*) *Solution behaviour for small times*

Our first calculations deal with the small-time evolution of the solution. The principal motivation for these simulations is to seek some confirmation that the underlying assumptions leading to the simpler pseudo-steady equations can be justified. Numerical results obtained using the complete model (2.10) and (2.11) for time scales of $O(\varepsilon)$ and distances of $O(\sqrt{D_r \varepsilon})$ from the boundary are displayed in figure 2. Very little substrate is converted over this short time scale while enzymes diffuse into the immediate neighbourhood of the boundary with consequent composite production. The composite concentration level at a point near the boundary increases in time and approaches the equilibrium level κ^{-1}; by contrast, the composite production rate function $es - \kappa\, c$ decays quickly to zero in both time and space. A detailed asymptotic analysis, see appendix A, indicates that

$$e(x', t') \sim \operatorname{erfc}\left(\frac{x'\sqrt{1+\kappa}}{2\sqrt{\kappa\, t'}}\right), \quad c(x', t') \sim \frac{1}{\kappa}\operatorname{erfc}\left(\frac{x'\sqrt{1+\kappa}}{2\sqrt{\kappa\, t'}}\right),$$

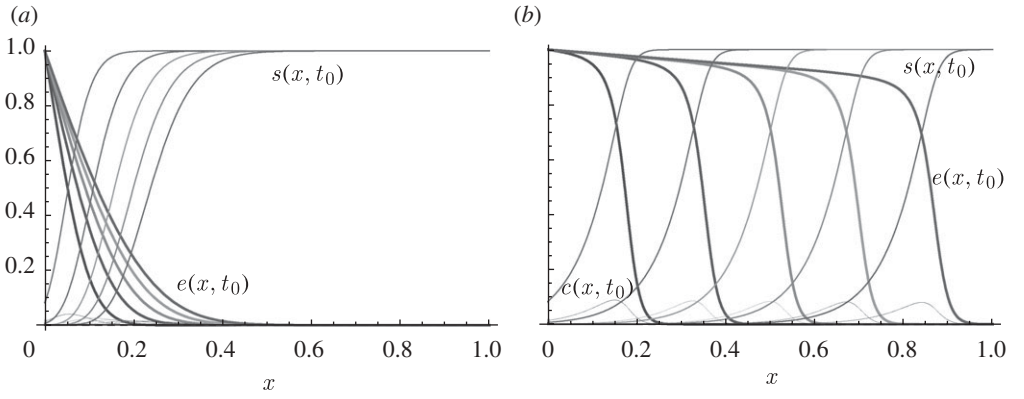

Figure 3. Moderate time solution behaviour. The lines denote the spatial forms of $e(x, t_0)$ (thick curves), $s(x, t_0)$ (medium curves) and $c(x, t_0)$ (thin curves) for the five times $t_0 = 3, 6, 9, 12$ and 15. Parameter values fixed as $\varepsilon = D_r = 10^{-4}$ and $\kappa = 6$. In (a) the diffusivity is constant so $\beta = 0$. In (b) $\beta = 6$.

as $(x', t') \to \infty$, where $x' = x/\sqrt{\varepsilon D}$, $t' = t/\varepsilon$ and erfc denotes the usual complementary error function; thus $c(x', t') \sim e(x', t')/\kappa$ as required by the pseudo-steady approximation.

Numerical simulations show that subsequently the composite production rate function remains zero to leading order so that the pseudo-steady model accurately describes the modification process for $t > O(\varepsilon)$.

(b) *Solution behaviour for* $t = O(1)$*: modification effects*

Results obtained using the complete model for time scales of order unity are displayed in figure 3. (Simulations were also performed using the pseudo-steady-state equations and these are graphically indistinguishable.) It is the small-scaled diffusivity $D_r \ll 1$ with $D_r e^{\beta} \geq 1$ (moderate to large β) case that is of particular relevance in the malting context, but the effect of substrate modification on the process is of primary interest, so we also consider the $\beta = 0$ (constant diffusivity) results. The contrast evident in figure 3 between the zero and the non-zero β problems shows that substrate modification effects can be dramatic.

In the constant diffusivity case, enzymes diffuse into the matrix triggering the reaction which occurs within the advancing modification front. This propagates into the region of low enzyme concentration, owing to a recycling of enzymes at the front, but this recycling is insufficient to maintain a constant speed; note the reduced composite concentration levels within the front at later times. Both the enzyme and the modification fronts slow as time advances (behaviour quite typical of diffusive systems), with the modification front outrunning the enzyme front in this case because of enzyme recycling.

In the $\beta = 6$ case, one observes linked travelling enzyme and substrate fronts (which are both sharp) accompanied by a composite wave, all of which travel at the same constant speed and with unchanging shape. In addition, the time t_m (loosely defined to be the time for the front to reach $x = 1$) is much reduced from $t_m \approx 69$ in the absence of modification, to $t_m \approx 16$, which is still much greater than the time required under uniform mixing conditions ($t_m \approx 4$) for the

prescribed parameters. Evidently, this is because the portion of the substrate that has been modified no longer offers substantial resistance to the transport of enzymes, so that the enzyme concentration remains almost constant immediately behind the moving front; in effect, enzymes are carried along and recycled within the propagating front thus maintaining its speed. Consistent with this is the almost constant enzyme concentration gradient behind the advancing front which provides the fixed enzyme flux required to preserve a constant speed and composite concentration levels within the front. This situation is also observed over the broad parameter ranges mentioned earlier and at the smaller diffusivities the fronts are sharper and move faster, as one might expect. In all these cases, the modification front speed remains almost constant as the front progresses and the enzyme and substrate profiles retain their shape. There is, however, a gradual reduction in front speed over much larger time and associated length scales; for details, see O'Brien (2004).

(*c*) *Approximate analytic solution for* $\beta \geq O(1)$

While the above numerical results provide us with some understanding of the behaviour of the modification front, an analytic result should provide much more insight. Here, we derive a simple approximate analytical result valid for the moderate to large values of β of interest, and use this to extract important front properties. Based on the computations, we anticipate a travelling wave solution of the form

$$e(x,t) = E(\zeta), \quad s(x,t) = S(\zeta), \quad c(x,t) = C(\zeta), \quad \text{where } \zeta = (x - X(t))/\sqrt{D_r} \tag{3.1}$$

(and $\dot{X} = \sqrt{D_r}\, V$); ζ is the scaled distance from the front centered on $X(t)$, moving with scaled front speed V, assumed constant. The computational work suggests that V is almost (but not exactly) constant; we will return to this issue later. We define the front position by $S = S_f$ at $X(t)$, so $S(0) = S_f$ defines $X(t)$. The pseudo-steady conservation equations (2.14)–(2.16) reduce to

$$V\frac{\partial S}{\partial \zeta} = SE, \tag{3.2}$$

$$-V\frac{\partial}{\partial \zeta}(E + C) = \frac{\partial}{\partial \zeta}\left(e^{\beta(1-S)}\frac{\partial E}{\partial \zeta}\right) \tag{3.3}$$

and

$$ES = \kappa C, \tag{3.4}$$

while the boundary and initial conditions require that $S \to 1$ and $E, E_\zeta, C \to 0$ as $\zeta \to \infty$ far ahead of the front. Behind the front, the boundary condition $e(0,t) = 1$ requires that $E(-X/\sqrt{D_r}) = 1$.

The total enzyme concentration equation (3.3) immediately integrates once to give

$$e^{\beta(1-S)}\frac{\partial E}{\partial \zeta} = -V(E + C),$$

where the constant of integration is fixed by imposing the conditions as $\zeta \to \infty$. Dividing this result by the substrate equation (3.2), rearranging and using

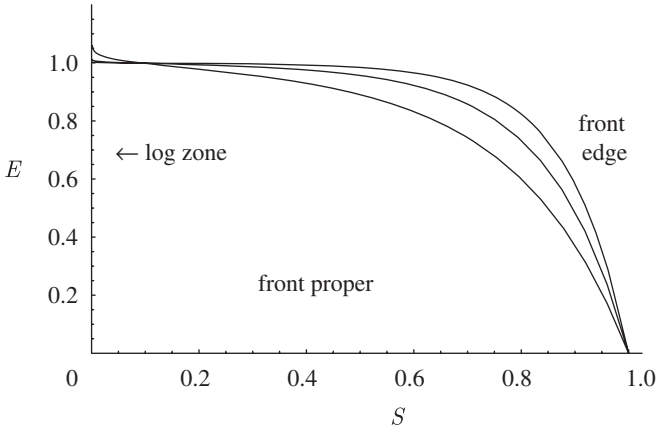

Figure 4. $E(S,\beta)$ as defined by equation (3.6). Note the linear front edge close to $S=1$, the flat front proper zone, and the thin logarithmic (enzyme diffusion) zone close to $S=0$. Results shown for $\beta=6$ (lower curve), 8 and 10. κ is large and $V=V_0$ as in equation (3.9).

equation (3.4) to eliminate C, we get

$$\frac{\mathrm{d}E}{\mathrm{d}S} = -V^2\, e^{-\beta(1-S)}\left(\frac{1}{S}+\frac{1}{\kappa}\right) \tag{3.5}$$

and a second integration gives

$$E(S) = V^2 e^{-\beta}\left[\mathrm{Ei}(\beta) - \mathrm{Ei}(\beta S) - \frac{e^{\beta}}{\kappa\beta}\{1 - e^{-\beta(1-S)}\}\right], \tag{3.6}$$

after satisfying required conditions as $\zeta \to \infty$; here $\mathrm{Ei}(z)$ denotes the exponential integral function (Abramowitz & Stegun 1964). The dependence $E(S)$ defined by (3.6) is plotted in figure 4.

The overall solution consists of three relatively distinct solution zones which are highlighted in figure 4, but can also be seen in the solution profiles shown in figure 5*b* below. Ahead of the front is a reasonably sharp-edged zone (the front edge) in which E varies almost linearly with S. Within this zone, the enzyme concentration E falls exponentially in x towards its far-field value of zero while the substrate concentration S is only exponentially different from its (scaled) asymptotic value of unity. Within the second zone (the front itself), E is almost constant, at a value (E_f say) that is slightly smaller than its boundary value 1, while S continues to reduce with distance to a value of order $1/\beta$ that defines the edge of this zone, see figures 4 and 5*b*. The $E(S)$ profile flattens with increasing β within this region and both reaction and nonlinear diffusion processes are active through these two front zones. Last comes the enzyme diffusion region. Here, the substrate concentration S is small and the diffusivity is now appreciable in size (at least for moderate to large β). Additionally, the reaction is almost complete and proceeds very slowly, so that a quasi-steady constant enzyme flux zone is to be expected. As is noted in appendix B, the logarithmic singularity in the $E(S)$ profile becomes significant within this zone and forces a linear dependence of E on x, with E changing from $E=E_f$ just behind the front edge to its boundary value $E=1$ at $x=0$, see figure 5*b*.

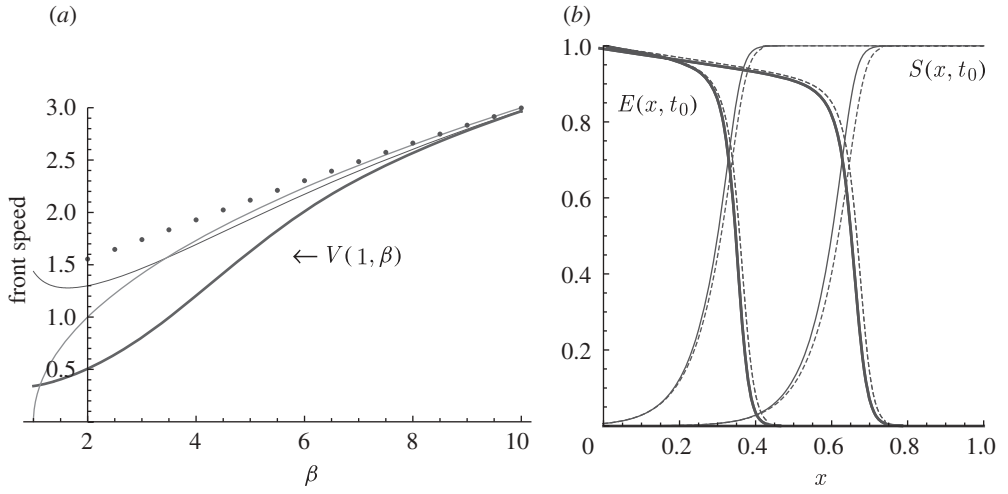

Figure 5. (*a*) Analytic front speed approximations. Plots of the scaled front speed $V(X,\beta)$ at $X=1$ obtained using equation (3.10) (thick curve), and of numerical results obtained using the complete model (dots). Also shown are the asymptotic front speed approximations $V_0(\beta)$ as in equation (3.9) (medium curve), and as in equation (3.12) (thin curve). (*b*) The approximate analytic solution for $E(x,t_0)$ (thick curves) and $S(x,t_0)$ (thin curves) for two fixed times t_0 ($D_r=10^{-3}, \beta=6$). Numerical results (dashed lines) are also superimposed.

As the substrate equation (3.2) can be inverted to give an implicit expression for $S(\zeta)$, namely

$$\int_{S_f}^{S} \frac{\mathrm{d}S'}{S'E(S')} = \frac{\zeta}{V}, \tag{3.7}$$

the two results (3.6) and (3.7) together (indirectly) determine the exact travelling wave solutions on the infinite domain satisfying the required boundary conditions as $\zeta \to \infty$. Solutions exist for all values of V so that merely asking that the model field equations should be satisfied by a travelling wave form is insufficient to tie down the front velocity. To determine V, we need to specify the enzyme input driving the travelling wave. We have $E=1$ at the boundary $x=0$ which, using equation (3.6), gives

$$V = e^{\beta/2}\left[\mathrm{Ei}(\beta) - \mathrm{Ei}(\beta S_0) - \frac{e^{\beta}}{\kappa\beta}\left\{1 - e^{-\beta(1-S_0)}\right\}\right]^{-1/2}, \tag{3.8}$$

where S_0 is the (as yet undetermined) substrate concentration at the boundary $x=0$.

It is at this stage we revisit our comment that V is not exactly constant; S_0 will not remain fixed but (very slowly) reduces as the front moves. On the face of it, this fact is in direct conflict with our original solution form (3.1) and so invalidates it, but the terms containing S_0 in (3.8) are only of the order $\exp[-\beta(1-S_0)]$ times the remaining dominant contributions in this expression and thus are relatively small for the moderate-to-large β situations of interest, see appendix B. If these

small terms are simply ignored, then

$$V \approx V_0 = e^{\beta/2}\left[\mathrm{Ei}(\beta) - \frac{e^{\beta}}{\kappa\beta}\right]^{-1/2}, \tag{3.9}$$

and, with this choice, $X(t) = \sqrt{D_r}\,V_0 t$ is determined and $E(S)$ and $S(\zeta)$ follow using equations (3.6) and (3.7). Hence, we have a complete parametric solution description which satisfies the solution requirements with only an exponentially small (in β) error.

In appendix B, we outline a more detailed asymptotic estimate for the substrate concentration level S_0 as a function of the front location X, and this has been used to determine an improved (quasi-steady) expression for the front speed given by

$$V \approx e^{\beta/2}\left[\mathrm{Ei}(\beta) - \gamma + \frac{(X-\Delta x)}{V_0\sqrt{D_r}} - \frac{e^{\beta}}{\kappa\beta}\right]^{-1/2}, \tag{3.10}$$

where

$$\Delta x = V_0\sqrt{D_r}\int_{S_b}^{S_f}\frac{\mathrm{d}S'}{S'E(S')} \tag{3.11}$$

is defined to be the front thickness and γ is Euler's constant. Here $S = S_b$ (of the order $1/\beta$) defines the back edge of the front; for algebraic convenience, we choose $S_b = 1/\beta$. While the terms in equation (3.10) extra to those in equation (3.9) are relatively small over propagation distances of unit order, this improved result does indicate a gradual reduction in speed as the front becomes further removed from the enzyme source; as mentioned earlier, the computations do show such speed reductions over large propagation distances. The associated enzyme and substrate profiles are obtained by substituting this expression for $V(X)$ into the previous results (3.6) and (3.7) for $E(S)$ and $S(\zeta)$, and upgrading X as the front progresses. Some of the results obtained in this way are displayed in figure 5, where computational results obtained using the complete model are also displayed for comparison. It can be seen from these figures that the analytic result accurately determines the front speed and structure for moderate to large values of β over length and time scales of interest. Somewhat surprisingly, the approximate analytic result even accurately predicts the front location; this occurs because the fully developed front emerges almost instantaneously.

It can be seen in figure 5*a* that the effect of front location on the front speed decreases rapidly with β and is almost negligible once $\beta > 8$. Thus, V_0 is an excellent approximation for the front speed for the cases of present interest. An even simpler (and only slightly less accurate) approximation for the front speed is given by

$$V_0 \approx \sqrt{\beta(1-1/(\kappa\beta))} \approx \sqrt{\beta} \quad \text{as } \beta \to \infty, \tag{3.12}$$

which is also plotted; we conclude that the front speed essentially increases like $\sqrt{\beta}$ for moderate to large β. This is a crude estimate but it proves useful for later comparisons. Our improved approximation (3.10) for V does not significantly affect the predicted enzyme and substrate profiles but now the boundary condition $E(0) = 1$ is accurately satisfied for the moving front over larger propagation distances.

The dependence of the front thickness Δx on the diffusivity variation parameter β is of some interest. The integral on the right-hand side of the expression (3.11) defining Δx remains almost constant for moderate to large β; in fact for $\beta \gg 1$, the integral evaluates to $\log(S_f/S_b) + O(1/\beta)$. Hence, the variation of front thickness with β arises primarily as a result of the $V_0(\beta)$ dependence and the rough estimate

$$\Delta x \approx 2\sqrt{\beta D_r} \tag{3.13}$$

(corresponding to $S_f/S_b = 8$) will be used later.

Further tests have shown that the results obtained above are relatively insensitive to the value of the complex production parameter κ. The primary effect is displayed in the front speed result (3.9), which indicates a small increase in speed for small κ. However, one would anticipate the production parameter κ to be moderate to large (corresponding to small complex concentration levels within the front), so that the front speed is virtually independent of the exact value of κ; numerical results confirm this conclusion.

For moderate to large β, we have already noted that the front takes a (scaled) time

$$t_m(D_r, \beta) = \frac{1}{\dot{X}} = \frac{1}{V\sqrt{D_r}} \approx \frac{1}{\sqrt{D_r \beta}}$$

to reach the end of a domain of unit length. When compared to the $1/D_r$ result relating to the $\beta = 0$ problem, it is apparent that for the values of β relevant to the malting application the time required for substrate conversion substantially decreases as a result of modification. When $D_r = 10^{-3}$, the scaled modification time is reduced by a factor of roughly five, from $t_m = 69.25$ in the absence of modification ($\beta = 0$) to $t_m = 12.9$ when $\beta = 6$. In unscaled terms, the modification time is

$$T_m = \tau_r t_m = \frac{\tau_r}{\sqrt{D_r \beta}} = L\sqrt{\frac{\tau_r}{D_0 \beta}}, \tag{3.14}$$

a result that clearly indicates that all three aspects of the process (reaction, diffusion and modification) play roles in fixing the modification time. In unscaled terms, the reaction zone thickness Δ (say) is approximately given by

$$\Delta = L\sqrt{D_r \beta}\,\Delta x = 2L\sqrt{D_r \beta} = 2\sqrt{\tau_r D_0 \beta}. \tag{3.15}$$

We remark that the two primary characteristics of the front, its speed and its thickness, are determined to first order by just two parameter combinations: an effective diffusivity $D_0\beta$ and the reaction time τ_r. Thus, in principle, measurement of the speed and thickness of the front can be used to determine these fundamental parameters of the problem. If $V_m = L/T_m$ is the unscaled propagation front speed, then equations (3.14) and (3.15) yield

$$D_0\beta = V_m \Delta/2 \quad \text{and} \quad \tau_r = \Delta/(2V_m). \tag{3.16}$$

(*d*) *Verification of the model*

In order to assess our predictions, we would ideally like to be able to appeal directly to experimental data concerning the diffusivities of glucanases in both unmodified and modified barley, together with the estimates of the reaction time τ_r. Unfortunately, we have been unable to locate such direct data, which is

perhaps not surprising because the reaction and diffusive process are inexorably linked in the natural process. Therefore, we proceed using some available indirect data.

Experimental measurements of the diffusion of water into barley grain can be used to estimate the diffusion coefficient D_0 for unmodified barley. The Stokes–Einstein equation (based on uninhibited Stokes flow around spheres) relates diffusivity levels in a given medium to the molecular weight of the diffusing molecules. In context, this suggests that

$$\frac{D_w}{D_0} = \left(\frac{M_\beta}{M_w}\right)^{1/3} \approx 17.7,$$

where $M_\beta \approx 10^5$ is the molecular weight of the β-glucanase molecule, $M_w = 18$ is the molecular weight of a water molecule, and D_0 and D_w are the associated diffusivities. Experiments by Holmberg *et al.* (1997) predict that it takes around 40 h for the moisture content of unmodified barley grain to rise from 10 to 45 per cent (corresponding to saturation); so that after applying the Stokes–Einstein factor (and noting that the diffusion time varies like $1/D$) one would anticipate a time scale of about $t_g = 29.5$ d for the diffusion of (non-reacting) glucanases through a barley grain. Assuming a diffusion length of $L = 4$ mm one can use the estimate $D_0 = L^2/(t_g(3.2)^2)$, which gives $D_0 \approx 0.61 \times 10^{-12}\,\mathrm{m^2\,s^{-1}}$. To derive estimates for the modified diffusivity $D_0 \exp(\mu s_0)$, we use the results of staining experiments in which partially modified barley grains are left in a solution of water and stain long enough for the solution to penetrate the modified (but not the unmodified) starch. This takes about 10 min, so if we use this as a characteristic penetration time we have that $\beta \approx \ln(40 \times 24 \times 60/10) = 8.6$ and $D_0 \exp(\mu s_0) \approx 3.5 \times 10^{-9}\,\mathrm{m^2\,s^{-1}}$.

Estimates for the reaction time τ_r can be made using the results of Bamforth & Martin (1983), who investigated β-glucanases at temperatures somewhat higher than typically encountered during malting. If an Arrhenius temperature dependence factor is used to account for this temperature difference, we infer that τ_r is just less than 1 hour. Combining this with the results for D_0 and β yields, a theoretical modification time T_m of about 1.2 days; somewhat shorter than, but within range of, the 4 or 5 days observed in practice. Note that the relevant time scales t_g (weeks) and τ_r (about 1 hour) that, together with β, determine the modification time differ by several orders of magnitude, so that our prediction for T_m (days) is surprisingly good. While it cannot be claimed that the result confirms the theory, it is legitimate to claim that the indications are good. Based on the above results, the scaled diffusivity parameter is calculated as $D_r = 0.13 \times 10^{-3}$ and $\beta = 8.6$. The reader will recall that our numerical illustrations were based on parameter values of $(D_r, \beta) = (10^{-3}, 6)$ and therefore we might expect the fronts in barley to be sharper than those seen in the above figures.

A second (and independent) attempt to validate the model was made based on front speed and thickness observations combined with the theoretical predictions (3.16). Front speed measurements are easily made and, although measurements of the front thickness should also be feasible, we have been unable to find any reports of such experiments. Instead we have visually examined some results taken from the literature. Oh & Briggs (1989) studied the interface between the modified and

the unmodified endosperm of the Maris Otter variety of barley using an electron micrograph. Their results suggest the front thickness to be somewhere between 100 and 200 μm. Selvig *et al.* (1986) produced a fluorescence photomicrograph of the front interface using Dansk Welam barley. Their images are harder to read but suggest a somewhat smaller front thickness, perhaps as short as 20 μm. Using 150 μm as representative, the result (3.16) yields a reaction time of about 2.2 h and $D_0 = 0.6 \times 10^{-12}\,\mathrm{m^2\,s^{-1}}$ (compared with the value $D_0 \approx 0.61 \times 10^{-12}\,\mathrm{m^2\,s^{-1}}$ obtained earlier). All one can claim is that these results are within the range of those obtained above, and the theoretical results obtained are consistent with the available observations. A more detailed description of the above estimates can be found in O'Brien (2004), but the authors believe that dedicated experiments are required to test the model assumptions and evaluate the model parameters in a consistent way.

4. Discussion

In this study, we have extended the Michaelis–Menten enzyme kinetics model to take into account the change in diffusive properties in the reacting substrate induced by an enzymic reaction. The model developed here represents the simplest possible model that incorporates the most obvious features of such situations and is hoped to be of broad applicability. When the diffusivity of the substrate is unaltered by the reaction, we have seen that the reaction propagates as a front moving with speed proportional to the inverse square root of time. In contrast, when the reaction substantially increases the diffusivity of the underlying substrate matrix, the front is sharp and moves with a near-constant speed that depends on the diffusivity variation parameter. These results seem to be qualitatively (and quantitively) consistent with barley modification experiments. Although space constraints prevent a thorough discussion here, studies also show that our theory is reasonably robust in the sense that the major results are not sensitive to the precise chosen form of the diffusion model (2.8). Rather, the predicted front speed (and thickness) is dependent only on the total change in diffusivity brought about by modification. The effect of a change in functional shape will only be seen within the internal structure of the front; a property that is quite common in many frontal propagation problems within the physical and biological sciences.

It is also noteworthy that the front speed as predicted by the model is insensitive to the strength of the enzyme source initiating the front, a result that may be used to test the validity of the model. As indicated earlier, this is a consequence of enzyme recycling at the front. Furthermore, investigations on a full three-dimensional grain model show that the eventual shape of the moving modification front as predicted by our model (2.14)–(2.16) is also relatively insensitive to the geometric shape of the enzyme source, a surprising result. In fact, the model predicts that an initially curved front quickly flattens out and travels as a planar front from the proximal to the distal end of the grain exactly as described above and observed in practice, see figure 1. This is again a consequence of the strongly nonlinear enzymic nature of the process. For further details, see O'Brien & Fowkes (2005). It is possible to change the source geometry by artificially injecting enzymes into the grain; such experiments may be useful

for testing the model. In a more general context, these results suggest that the constant speed travelling fronts are likely to be set up in circumstances in which the effect of the reaction is to greatly increase the diffusivity of the underlying matrix. Apart from enzyme-related contexts, this is likely to be the case in cooking contexts, for example, the cooking of a rice grain.

Of course, the actual diffusion processes that occur within a barley grain during modification are more complex than is suggested by the simple model (2.8) adopted here. In practice, the enzymes move in an environment that is both complex and continuously changing. Moreover, the diffusion will not be passive owing to the interactions with other cellular components such as receptors, antigens or other enzymes. In theory, one might attempt to account for the detailed interactions using a microscopic model (involving ensemble averages of intermolecular potentials and hydrodynamic interactions) or a semi-microscopic Stokes–Einstein model (involving cross-diffusion tensors with associated fluxes). Such models, though more detailed and thus initially more attractive, would necessarily involve more quantities that are unlikely to be measurable especially within the confined space of the reaction front. In short, such models would probably be untestable in the present context. By contrast, and as suggested above, our macroscopic model, though simplistic, is enough to estimate the front speed and its thickness and indicates some of the global features of the process by which an enzyme invades a substrate whose diffusivity increases dramatically as a result of the reaction.

The authors would like to thank John King for pointing out an inconsistency in an earlier modification model, and Andrew Bassom whose suggestions concerning presentation greatly improved readability.

Appendix A. Small-time asymptotics

We expect the introduction of enzymes at $x=0$ when $t=0$ to result in an initial rapid response (on a time scale of order ε) in the neighbourhood of $x=0$. This should lead quickly to a pseudo-steady state in which $se-\kappa c=0$ to first order in ε and on this time scale we anticipate that enzymes diffuse over a distance of $O(\sqrt{Dt})$.

To examine this proposition, we rescale the complete one-dimensional model equations (2.10) and (2.11) by putting $t'=t/\varepsilon$ and $x'=x/\sqrt{D\varepsilon}$. With these definitions, the model equations become

$$\frac{\partial s}{\partial t'}=\varepsilon(Rc-se), \tag{A 1}$$

$$\frac{\partial(e+c)}{\partial t'}=\frac{\partial}{\partial x'}\left[\exp(\beta(1-s))\frac{\partial e}{\partial x'}\right] \tag{A 2}$$

and

$$\frac{\partial c}{\partial t'}=se-\kappa c, \tag{A 3}$$

while the appropriate boundary conditions are

$$e(0,t')=1 \quad \text{together with } e(x,0)=c(x,0)=0 \quad \text{and} \quad s(x,0)=1 \tag{A 4}$$

with no input as $x \to \infty$. Thus, to first order in ε over a time scale $t' = O(1)$ we have that $\partial s/\partial t' = 0$ and then initial condition (A 4) implies $s = 1$. To first order in ε, the remaining equations then yield

$$\frac{\partial(e+c)}{\partial t'} = \frac{\partial^2 e}{\partial x'^2} \tag{A 5}$$

and

$$\frac{\partial c}{\partial t'} = e - \kappa c, \tag{A 6}$$

this constant coefficient equation set can be solved using Laplace transforms. If we define the transform quantities $\mathcal{E}(x,p)$ and $\mathcal{C}(x,p)$ in the usual way so that

$$\{\mathcal{E}(x,p), \mathcal{C}(x,p)\} \equiv \int_0^\infty \exp(-pt)\{e(x,t), c(x,t)\}\,\mathrm{d}t,$$

system (A 5) and (A 6) has the solution

$$\mathcal{E} = \frac{1}{p}\exp\left\{-x'\sqrt{p[1+1/(p+\kappa)]}\right\} \quad \text{and} \quad \mathcal{C} = \frac{\mathcal{E}}{(p+\kappa)}, \tag{A 7}$$

so that

$$\mathcal{E} - \kappa\mathcal{C} = \frac{\exp\left\{-x'\sqrt{p[1+1/(p+\kappa)]}\right\}}{\kappa + p}, \tag{A 8}$$

after applying the initial and boundary conditions (A 4). When $t' \ll 1$, the inversion formula gives

$$e(x',t') \sim \operatorname{erfc}\left(\frac{x'}{2\sqrt{t'}}\right) \quad \text{and} \quad c(x',t') \sim \int_0^{t'} \operatorname{erfc}\left(\frac{x'}{2\sqrt{u'}}\right)\mathrm{d}u',$$

where we have ensured that the initial conditions are satisfied. On the other hand, when $t \gg 1$, then

$$e(x',t') \sim \operatorname{erfc}\left(\frac{x'\sqrt{1+\kappa}}{2\sqrt{\kappa t'}}\right) \quad \text{and} \quad c(x',t') = \frac{1}{\kappa}\,e(x',t');$$

evidently $e - \kappa c \to 0$ as $t' \to \infty$ as required by the pseudo-steady approximation. More accurately, it can be shown that

$$e(x',t') - \kappa\, c(x',t') \sim \frac{x'\sqrt{1+\kappa}}{2\sqrt{\pi}\,(\kappa t')^{3/2}}\,\exp\left\{-\frac{\kappa\,(x')^2}{4(1+\kappa)\,(t')^2}\right\}.$$

Appendix B. Improved front speed estimates

Here, we sketch the derivation of the improved estimate (3.10) for the front speed. We begin by taking the travelling wave $E(S)$ relationship (3.6) rewritten in the form

$$E(S) = V^2 e^{-\beta}\left[\{\mathrm{Ei}(\beta) - \mathrm{Ei}(\beta S)\} - \frac{e^\beta}{\kappa\beta}(1 - e^{-\beta(1-S)})\right], \tag{B 1}$$

for convenience. We remark that $\mathrm{Ei}(z) \sim e^z/z$ for $z \gg 1$ and $\mathrm{Ei}(z) \sim \log(z)$ for $0 < z \ll 1$, so that for moderate to large β and $1/\beta < S < 1$ the $\mathrm{Ei}(\beta)$ term in equation (B 1) is dominant. However, for $S < 1/\beta$ the logarithmic singularity associated with the $\mathrm{Ei}(\beta S)$ part of the solution becomes important. Note also that the terms outside the braces are relatively small and do not significantly affect our subsequent workings.

If the front is already fully developed (so that substrate levels at the boundary are at most of $O(\beta^{-1})$), then we can approximate $E(S)$ as in equation (B 1) close to the boundary by the series expansion

$$E(S) = V^2\, e^{-\beta}\left[\{\mathrm{Ei}(\beta) - \ln(\beta S_0) - \gamma\} - \frac{e^{\beta}}{\beta\kappa}\right] + O(\beta S, e^{-\beta}), \tag{B 2}$$

where γ is Euler's constant (Abramowitz & Stegun, 1964).

To estimate the substrate level S_0 at the boundary as a function of front location using equation (3.7), we first split the moderate S (wave front) contribution to the integral defining $S(\zeta)$ from the associated small-S contribution to give

$$\begin{aligned}\int_{S_f}^{S} \frac{\mathrm{d}S'}{S'E(S')} &= \int_{S_f}^{S_b} \frac{\mathrm{d}S'}{S'E(S')} + \int_{S_b}^{S} \frac{\mathrm{d}S'}{S'E(S')},\\ &= -\frac{\Delta\zeta}{V} + \int_{1/\beta}^{S} \frac{\mathrm{d}S'}{S'E(S')},\end{aligned}$$

where $S = S_b\,(= O(\beta^{-1}))$ defines the rear of the front, and where

$$\Delta\zeta \equiv V\int_{S_b}^{S_f} \frac{\mathrm{d}S'}{S'E(S')} \tag{B 3}$$

can be thought of as the scaled thickness of the front. The $S \ll 1$ contribution to the integral can be approximated by replacing E by its value (unity) on the boundary and the integral evaluated to give

$$\ln(\beta S) \sim \frac{\zeta + \Delta\zeta}{V} \quad \text{for } S < \frac{1}{\beta},$$

after rearranging, and where we have chosen $S_b = 1/\beta$. We substitute this expression for $\log(\beta S)$ into the approximation (B 2) for $E(S)$ obtained earlier to obtain an improved estimate for enzyme concentration levels near the boundary

$$E(\zeta) \approx V^2\, e^{-\beta}\left[\mathrm{Ei}(\beta) - \gamma - \frac{\zeta + \Delta\zeta}{V} - \frac{e^{\beta}}{\kappa\beta}\right] \quad \text{for } \zeta \ll 1.$$

The boundary condition $E = 1$ and $S = S_0$ at $x = 0$ can now be applied to give

$$V \approx e^{\beta/2}\left[\mathrm{Ei}(\beta) - \gamma + \frac{(X - \Delta x)}{V_0\sqrt{D_r}} - \frac{e^{\beta}}{\kappa\beta}\right]^{-1/2} \tag{B 4}$$

(cf. (3.10)), where $\Delta x \equiv \Delta\zeta\sqrt{D_r}$ is the front thickness and where we have replaced V by V_0 in the denominator with no further loss in accuracy.

References

Abramowitz, M. & Stegun, I. A. 1964 *Handbook of mathematical functions*. New York, NY: Dover Publications.

Bamforth, C. W. & Martin, H. L. 1983 The degradation of β-glucan during malting and mashing: the role of β-glucanase. *J. Inst. Brew.* **89**, 303–307.

Briggs, D. E. & MacDonald, J. 1983 Patterns of modification in malting barley. *J. Inst. Brew.* **89**, 260–273.

Briggs, G. E. & Haldane, J. B. S. 1925 A note on the kinetics of enzyme action. *Biochem. J.* **19**, 338–339.

Holmberg, J., Hamalainen, J. J., Reinikainen, P. & Olkku, J. 1997 A mathematical model for predicting the effects of the steeping programme on water uptake during malting. *J. Inst. Brew.* **103**, 177–182.

Landman, K. A. & Please, C. P. 1999 Modelling moisture uptake in a cereal grain. *IMA J. Math. Appl. Bus. Ind.* **10**, 265–287.

McGuinness, M. J., Please, C. P., Fowkes, N., McGowan, P., Ryder, L. & Forte, D. 2000 Modelling the wetting and cooking of a single cereal grain. *IMA J. Math. Appl. Bus. Ind.* **11**, 49–70.

O'Brien, R. T. 2004 Modelling the transport and reaction of enzymes in germinating barley. PhD thesis, School of Mathematics and Statistics, University of Western Australia, Crawley, Australia.

O'Brien, R. T. & Fowkes, N. 2005 Modification patterns in germinating barley — malting II. *J. Theor. Biol.* **233**, 315–325. (doi:10.1016/J.Jtbi.2004.10.010)

Oh, S. Y. & Briggs, D. E. 1989 Modification in malting barley. *J. Inst. Brew.* **95**, 83–88.

Palmer, G. H. 1983 Theories of endosperm modification. *J. Inst. Brew.* **89**, 156–159.

Selvig, A., Aarnes, H. & Lie, S. 1986 Cell-wall degradation in the endosperm of barley during germination. *J. Inst. Brew.* **92**, 185–187.